Indian Journal of Chemistry
Vol. 59A, July 2020, pp. 887-894

A sensitive and selective fluorescence sensing of bisphenol A based on magnetic Fe_3O_4@SiO_2@QDs@MIPs nanoparticles

Yafang Zhang, Xiaolong Wei & Zhihua Wang*

Key Laboratory of Bioelectrochemistry & Environmental Analysis of Gansu Province, College of Chemistry & Chemical Engineering, Northwest Normal University, Lanzhou, 730070, P. R. China
Email: zhwang@nwnu.edu.cn

Received 11 November 2019; revised and accepted 02 May 2020

A flexible magnetic and fluorescent sensing for the recognition and detection of bisphenol A (BPA) based on a hybrid magnetic Fe_3O_4@silica nanoparticle@Mn:ZnS quantum dots@molecularly imprinted polymers nanoparticles (Fe_3O_4@SiO_2@QDs@MIPs NPs) has been designed. Because of the high selectivity of MIPs, the strong fluorescence property of Mn:ZnS QDs, good magnetism of Fe_3O_4 and good water solubility of SiO_2, the Fe_3O_4@SiO_2@QDs@MIPs NPs can effectively detect BPA effectively in human urine. In the presence of BPA, a new compound is produced via the amino group of Fe_3O_4@SiO_2@QDs@MIPs NPs and the hydroxyl group of BPA, the energy of the QDs is transferred to the compound, which led to fluorescence quenching. The relative fluorescence intensity has decreased linearly with the increasing of BPA concentration in the range 50 to 700 ng/mL and the detection limit is found to be 1.6 ng/mL. In addition, the sensor has shown a strong selectivity with an imprinting factor of 8.7 and distinguished selectivity is also exhibited to BPA over other possibly competing molecules. On the basis of the merits of the Fe_3O_4@SiO_2@QDs@MIPs NPs, the sensor can be applied to detect BPA in human urine sample successfully.

Keywords: Bisphenol A, Fluorescence analysis, Mn-doped ZnS quantum dot, Molecularly imprinted polymers, Fe_3O_4 nanoparticles

Bisphenol A (BPA, 2,2-bis(4-hydroxyphenyl)propane) is a very important derivative of acetone and phenol, one of the representative endocrine-disrupting chemicals (EDCs), which is widely used to make plastic products of polycarbonate plastics, polystyrene resins, flame retardants, epoxy resins, and other featured products, and it's also commonly used in daily supplies such as baby bottles, toiletry, plastainer, etc[1-3]. When the materials are exposed to high temperatures, the unstable and lipophilic compound BPA may be transferred to food and water by food contact materials, or get into the environment through waste water from the plastics manufacturing industry[4]. As one of known endocrine disrupters, BPA have negative effect on endocrine system of human, and can interfere with central nervous system, immune system, thyroid function, reproduction system and endocrine pancreas [5,6] and the devil of it is that it can mimic the body's own hormones and increase the risk of cancer[7,8]. So it is extremely desirable to determine trace amounts of BPA and it is hopeful for confirming diagnosis of the disease.

To date, a lot of analytical methods have been successfully developed for the detection of BPA, the most frequently-used methods are high performance liquid chromatography[9], liquid chromatography-mass spectrometry[10], liquid chromatography-tandem mass spectrometry[11], gas chromatography-mass spectrometry[12], liquid chromatography-coulometric detection[13], liquid chromatography-fluorescence detection[14,15], liquid chromatography-UV detection[16], electrochemical sensors[17-23], and enzyme-linked immunosorbent assays[24, 25]. Although there are lots of chromatography methods for BPA detection, the methods require professional operators, high test charge, expensive equipment, complex sample pre-treatment and considerable time, it is very important to develop new ways for detecting BPA. With great promise way the electrochemical methods to meet what was said above requirements, but those sensors normally along with low sensitivity, and enzyme analysis method with low stability. Compared with the above methods, fluorescence analysis is an attractive analytical method. In recent years, various chemical sensors of using fluorescence analysis have been widely utilized and accepted, because of the mainly features of high sensitivity, selectivity and ease of use[26-28]. In the meantime, molecularly

imprinted polymers (MIPs) with high selectivity and stability, easy preparation and low cost have flourished in the field of chemo/biosensors analysis[29-31]. The principle behind the co-polymerization of functional monomers and cross-linking monomers in the presence of an imprinted molecule is similar to that of antigen-antibody reactions[32,33]. The application of MIPs in fluorescence sensors have been reported by some researchers[34-37] and the surface molecularly imprinted polymers (SMIPs) coupled with quantum dots (QDs) based sensors have developed rapidly[38,39]. Recently, the fluorescent approach that involves the nano-materials, especially magnetic Fe_3O_4 NPs had been used for the detection of BPA. These methods using super paramagnetic magnetic materials have unique advantages compared with other spectral analysis methods[40]. For example, Meng-Ke Li and co-workers[41] established a fluorescence probe based on amino-functionalized magnetic Fe_3O_4 and AHN-labeled aptamer detecting BPA. Furthermore, Amal et al.[42] designed a magnetic molecularly imprinted polymer for the selective recognition of methyl parathion.

As far as we know, there are rarely reports with fluorescent sensors to detect BPA, combining with magnetic Fe_3O_4 NPs, QDs and MIPs. Inspired by the above mentioned researches, a fluorescent probe based on Mn^{2+} doped ZnS QDs and magnetic MIPs via a sol-gel polymerization process was designed for selective recognition and sensitive detection of BPA. The relative fluorescence intensity was decreased linearly with the increase in the concentration of BPA in the range of 50-700 ng/mL, with the limit of detection 1.6 ng/mL.

Materials and Methods

Reagents and samples

BPA was purchased from Energy Chemical Co. Ltd. Acryl amide (AM) was purchased from Sinopharm Chemical Reagent Co. Ltd. Zinc sulfate heptahydrate ($ZnSO_4{\cdot}7H_2O$) was obtained from Aladdin (Shanghai, China). Manganese(II) chloride tetrahydrate ($MnCl_2{\cdot}4H_2O$) was obtained from Saen (Shanghai, China). Sodium sulfide ($Na_2S{\cdot}9H_2O$) was obtained from Shuangshuang (Yantai China). Ferric chloride ($FeCl_3{\cdot}6H_2O$), ferrous sulphate ($FeSO_4{\cdot}7H_2O$), and ammonium nitrate ($NH_4{\cdot}NO_3$) were purchased from Tianhe (Guangdong, Chaina). Cetyltrimethylammonium bromide (CTAB), tetraethoxysilane (TEOS), dimethyl sulfoxide (DMSO), ethanol, acetonitrile and sodium hydroxide were obtained from Kermel (Tianjin, China). (3-mercaptopropyl) trimethoxysilane (KH-590), 3-mercaptopropionic acid, (3-aminopropyl) triethoxysilane (APTES) and (3-isocyanatopropyl)-triethoxysilane (ICPTES) were obtained from Aladdin (Shanghai, China). Ultrapure water was used throughout the studies. Other reagents were of analytical grade and used without further purification. Fresh human urine samples were available from Northwest Normal University Hospital.

Instrumentation

Fluorescence spectra were obtained on a RF-5301 spectrofluorophotometer (Japan, Shimadzu Co.). Scanning electron microscopy (SEM) images were made on a Carl Zeiss SUPRA 55VP (Germany, Oberkochen Co.). Transmission electron microscopy (TEM) images were carried out on FEI Tecnai F20 and FEI Tecnai G^2 F20 Stwin operating at 200 kV and 5 kV (America, FEI Co.). UV-visible absorption spectra were absorbed by using an UV-8453 Spectrophotometer (Japan, Agilent Co.). FTIR was recorded on an Alpha Centauri FTIR spectrometer (America, Mattson Co.,). Energy Dispersive Spectrometer (EDS) was performed on equipped with Gatan832 at an accelerating voltage of 5 kV (America, EDAX Co.). Powder X-ray diffraction (XRD) spectra were obtained with the use of an AXS D8-Advanced diffractometer (Germany, Bruker Co.).

Synthesis of the Mn:ZnS QDs, Fe_3O_4 NPs and Fe_3O_4@SiO_2 NPs

The preparation of Mn: ZnS QDs were according to the reports[43,44]. Fe_3O_4 NPs were prepared on the basis of literature[45] with minor modification. Firstly, Iron(III) acetylacetonate (0.706 g, 2 mmol) was dissolved in a mixture of benzyl ether (10 mL) and oleylamine (10 mL). Secondly, the solution was heated at 120 °C for 1 h and then the mixture was heated at 300 °C for 2 h in nitrogen atmosphere. Then, the black-brown mixture was cooled to room temperature. The resulted products were washed with ethanol five times, separated from the solution with a magnet and centrifuged (6000 rpm) soon afterwards. Finally, the product was redispersed in n-hexane.

The Fe_3O_4 NPs (0.2 g) was added to 10 mL, 0.1 mol/L CTAB solution by ultrasound 30 min and stirring 30 min with repeating three times. 0.1 mol/L NaOH solution was added to adjust the pH of the solution (8.5). The reaction was carried out under the water bath in 40 °C for about 24 h. Then, the TEOS

(1.5 mL) was added by dropwise into the mixture while stirring, and the mixture was stirred for 24 h at room temperature. The products were washed by ultrapure water time after time and separated from the solution by centrifuged (8000 rpm) soon afterwards. Finally, the Fe_3O_4@SiO_2 NPs were dried under vacuum in 55 ℃.

Preparation of Fe_3O_4@SiO_2@QDs@MIPs NPs

The Fe_3O_4@SiO_2@QDs@MIPs NPs synthesis could be divided into two steps. Firstly, the Fe_3O_4@SiO_2 (0.2 g), Mn:ZnS QDs (0.1 g), ethanol (1.0 mL) and $NH_3{\cdot}H_2O$ (150 μL), KH-590 (200 μL) were added to the water, while stirring at room temperature for 12 h. Secondly, the BPA (0.02 g), APTES (100 μL), AM (0.12 g) and ICPTES (100 μL) were added to the solution of first step, and the mixture was stirred at room temperature in a nitrogen atmosphere for 4 h. Then, TEOS (200 μL) and NaOH solution (2 mol/L, 1 mL) were added and the mixture was sealed and kept under stirring for 7 h under nitrogen atmosphere. After the reaction was finished, the template molecule was washed with acetonitrile/ethanol (2:8, v/v) twice to remove the templates. In the end, the product was centrifuged (8000 rpm), washed with ethanol three times and dried under vacuum. The Fe_3O_4@SiO_2@QDs@MIPs NPs were obtained. The Fe_3O_4@SiO_2@QDs@NIPs NPs were synthesized similarly to the Fe_3O_4@SiO_2@QDs@MIPs NPs, except that the template did not exist in the polymerization.

Fluorescence experiment

The fluorescence spectra of the Fe_3O_4@SiO_2@QDs@MIPs NPs and Fe_3O_4@SiO_2@QDs@NIPs NPs were obtained under a photomultiplier tube voltage of 550 V. The excitation and emission wavelengths were 350 nm and 590 nm, respectively. The scanning wavelength scope was 500 ~ 700 nm. Every spectrum was obtained with three parallel scans with slit width was 7 nm, the scan speed was 240 nm/min. The various concentrations of BPA solutions (pH=7.5) were added to 0.1 mg/mL Fe_3O_4@SiO_2@QDs@MIPs NPs solution and the volume ratio was 1:1. The control experiments of the Fe_3O_4@SiO_2@QDs@NIPs NPs were carried out as the same process. Each test were run three times and taken the mean to eradicate any discrepancies.

Detection of BPA in human urine samples

The urine samples was stored in refrigerator (-18 °C). The urine was thawed with heat and diluted 10 times by water. The various concentrations of BPA in samples ranging from 50 to 700 ng/mL were obtained by adding different amounts of BPA to the diluted urine. The 0.1 mg/mL Fe_3O_4@SiO_2@QDs@MIPs NPs solution was added into the diluted urine spiked with BPA in a volume ratio of 1:1. The mixture was centrifuged (6000 rpm) after incubating for 4.5 min, and the Fe_3O_4@SiO_2@QDs@MIPs NPs were dispersed into water (pH=7.5) for the fluorescent analysis of BPA.

Results and Discussion

Synthesis of Fe_3O_4@SiO_2@QDs@MIPs NPs

The typical synthesis process of Fe_3O_4@SiO_2@QDs@MIPs NPs was depicted in Scheme 1. The process would consist of three steps: the preparation of Mn:ZnS QDs, the synthesis of Fe_3O_4 NPs, and the combination of the two materials to prepare the Fe_3O_4@SiO_2@QDs@MIPs NPs. Choosing BPA as template, the APTES and AM used as functional monomer reacted non-covalently with the template (BPA) through hydrogen bonds[46], the template BPA could be introduced on the surface of the uniform polymers[47]. ICPTES as assistant functional monomer, CTAB as surface active agent, and TEOS as cross-linker, the Fe_3O_4@SiO_2@QDs@MIPs NPs were formed by sol-gel process. Fe_3O_4 NPs surface were wrapped in SiO_2 NPs during the polymerization, QDs were modified on the surface of SiO_2 NPs, and a film of the molecularly imprinted polymers (MIPs) was formed on the surface of materials. After removal of the templates, the specific recognition sites were obtained on the surface of the composites. In order to get more binding sites and improve the sensitivity of detecting

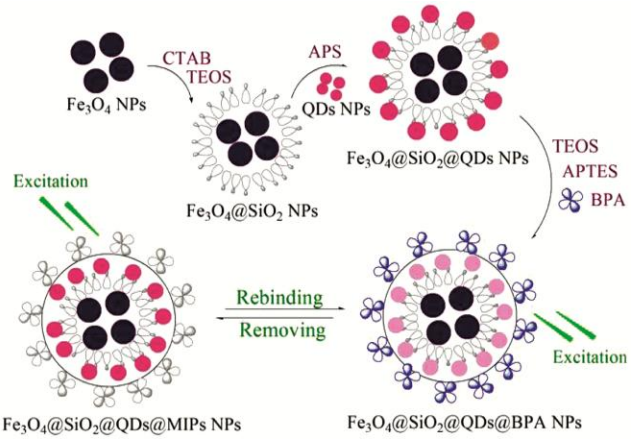

Scheme 1 — A schematic representation for the process of construction of Fe_3O_4@SiO_2@QDs@MIPs NPs.

for BPA, AM and APTES were selected as the main functional monomer, ICPTES was added as ancillary functional monomer because they could form H-bond to the BPA. Molecular imprints can keep a permanent memory for the template that makes the imprinted polymer to recombine the template selectively in the presence of structural analogs. Mn^{2+} was doped into the ZnS QDs to enhance its luminescence property, and the fluorescence emitting of the Mn:ZnS QDs could be quenched when the Fe_3O_4@SiO_2@QDs@MIPs were recombined to BPA. The particles of Fe_3O_4@SiO_2@QDs@MIPs could be separated expediently with external magnetic field for recovery.

Characteristic of Fe_3O_4@SiO_2@QDs@MIPs NPs

The TEM images of Mn:ZnS QDs and Fe_3O_4 NPs are demonstrated in Fig. 1a and 1b, respectively. The average diameters of spherical Mn:ZnS QDs and Fe_3O_4 NPs particles are 6 nm and 10 nm, respectively. The morphological analysis of Fe_3O_4@SiO_2@QDs@MIPs NPs and Fe_3O_4@SiO_2@QDs@NIPs NPs were observed by SEM and depicted in Fig. 1c and 1d. Huddles of Fe_3O_4@SiO_2@QDs@MIPs NPs and Fe_3O_4@SiO_2@QDs@NIPs NPs with the size of 200 nm are observed. The crystalline structure and purity of the Mn:ZnS QDs were studied by the XRD. A face-centered cubic structure with peaks assigned to (311), (220) and (111) has seen from Fig. 1e, which indicates that the formation of Mn:ZnS QDs. Moreover, Fe_3O_4 NPs, Fe_3O_4@SiO_2 NPs and Fe_3O_4@SiO_2@QDs@MIPs NPs were certified by EDS, the results are given in Supporting Data (Fig S1), which confirm the successful formation of Fe_3O_4 NPs Fe_3O_4@SiO_2 NPs and Fe_3O_4@SiO_2@QDs@MIPs NPs.

The FTIR of Fe_3O_4 NPs, Fe_3O_4-@SiO_2@QDs@MIPs and Fe_3O_4@SiO_2@QDs@NIPs are shown in Fig 1f. An intensive peak is observed at 589 cm^{-1}, which is due the vibration of Fe-O band (curve 1), a wide and intensive peak is emerged at 1109 cm^{-1} (curve 1, 2), due to asymmetric vibration of the Si-O-Si band, and the peaks at 794 and 467 cm^{-1} are attributed to the vibration of the Si-O band. The peaks at 3405 cm^{-1} (N-H band) and 2976 cm^{-1} (C-H band) belong to the aminopropyl group and the peak at 2976 cm^{-1} is the (C-H) stretching vibration. The Fe_3O_4@SiO_2@QDs@NIPs have a similar feature (curve 3) with Fe_3O_4@SiO_2@QDs@MIPs except the peak at 3405 cm^{-1} (N-H band) is not observed, which confirmed that the BPA has been imprinted on the silica surface successfully.

The fluorescence stability of the Fe_3O_4@SiO_2@QDs@MIPs NPs

The stability of fluorescence material should be considered. The fluorescence intensity of Mn:ZnS QDs and Fe_3O_4@SiO_2@QDs@MIPs NPs were studied (Fig. S2a). It was found that the fluorescence intensity of Mn:ZnS QDs (curve 1) and Fe_3O_4@SiO_2@QDs@MIPs NPs (curve 2) almost kept

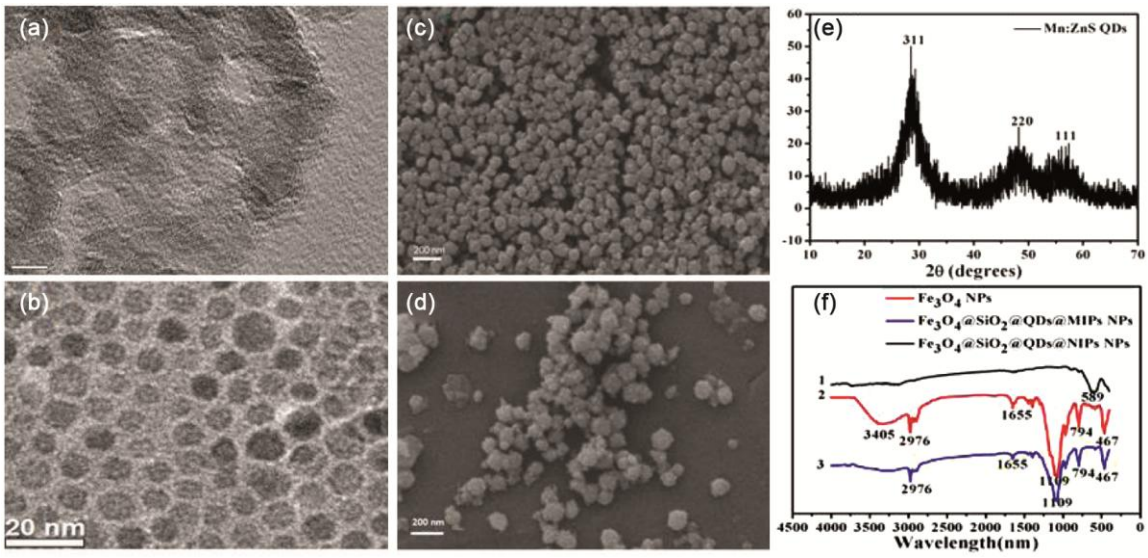

Fig. 1 — TEM images of (a) Mn:ZnS QDs and (b) Fe_3O_4 NPs; SEM images of (c) Fe_3O_4@SiO_2@QDs@MIPs NPs and (d) Fe_3O_4@SiO_2@QDs@NIPs NPs; XRD plot of (e) Mn:ZnS QDs; Fourier transform infrared spectra of Fe_3O_4 NPs (f, 1), Fe_3O_4@SiO_2@QDs@MIPs NPs (f, 2) and Fe_3O_4@SiO_2@QDs@NIPs NPs (f, 3).

the same in an hour, and the relative standard deviation (RSD) was less than 0.3%, which indicates the very good stability of the prepared materials

Incubation time

The fluorescent intensity of Fe_3O_4@SiO_2@QDs@MIPs NPs was decreased sharply when BPA was added and was kept stable after 4.5 min. The results are shown in Fig. S2b. So, 4.5 min was chosen for the incubation time.

Effect of pH

The pH of solution has a very important influence on the fluorescent properties of materials. The results are displayed in Fig. S2c. It is found that the fluorescent intensity of Fe_3O_4@SiO_2@QDs@MIPs NPs was increased with the increasing of pH at the beginning and reached the maximum when pH was 7.5, then the fluorescent intensity was decreased with the increasing of pH. The reason could be Mn:ZnS QDs reacted with acid to generate H_2S in acid solution[43], and the imprinted silica layers could be ionized in the basic solution that led the interaction between BPA and the imprinting sites to weak. So, pH=7.5 was chosen for the experiments.

Selectivity of Fe_3O_4@SiO_2@QDs@MIPs NPs

Influences of coexistent substances on the fluorescent intensity of the prepared materials were examined. The results of the comparison are shown in Fig. S2d. Several analogues including benzidine, benzophenone, hydroquinone, resorcinol, and BPB were selected. Compared with the blank solution, the fluorescence intensity of Fe_3O_4@SiO_2@QDs@MIPs NPs had no obvious differences when the analogues were added in the solution, and a remarkable decreasing of fluorescence intensity was observed when BPA was added, while the fluorescence intensity of Fe_3O_4@SiO_2@QDs@NIPs NPs had no obvious differences when BPA and the analogues were added in the solution. It showed Fe_3O_4@SiO_2@QDs@MIPs NPs having a predetermined selectivity for template were able to recognize BPA from the structurally similar molecule. It indicated that the Fe_3O_4@SiO_2@QDs@MIPs NPs had good selectivity to BPA and could be used to detect BPA in real sample.

At the same time, the influence of several substances and inorganic ions in human body on the determination of BPA were also examined. The solutions consisted of 700 ng/mL BPA and interfering species. The results indicated that a 20-fold excess of K^+, Na^+, Ca^{2+}, Mg^{2+}, Cl^- and 10-fold excess of urea, amylum, glucose, maltose, glycine, glutathione had no significant influence on the measurement of BPA.

Fluorescent measurement

The fluorescent intensity of the prepared materials decreased with the addition of BPA (Fig. 2a and 2c). A remarkable decreasing of fluorescence intensity of Fe_3O_4@SiO_2@QDs@MIPs NPs was observed and while it was a minor change for Fe_3O_4@SiO_2@QDs@NIPs NPs when BPA was added in the solution. It could be explained by Stern-Volmer law below.

$$F_0/F = KsvCq + 1$$

Where, F is the fluorescence intensity in the presence of BPA, F_0 is the fluorescence intensity in the absence of BPA, K_{SV} is the Stern-Volmer constant and Cq is the concentration of BPA. The results are shown in Fig. 2b and 2d. The linear regression equation for Fe_3O_4@SiO_2@QDs@MIPs NPs is F_0/F=0.0035Cq-0.0976, with a correlation coefficient of 0.9921, the liner range is 50 to 700 ng/mL and the detection limit is 0.16 ng/mL; the linear regression equation for Fe_3O_4@SiO_2@QDs@NIPs NPs is F_0/F=0.0004Cq+0.0261, the ratio of $K_{sv,\ MIP}$ to $K_{sv,\ NIP}$ is defined as the imprinting factor (IF), IF = 8.7 can be obtained. It indicated that the Fe_3O_4@SiO_2@QDs@MIPs NPs, compared with the Fe_3O_4@SiO_2@QDs@NIPs NPs, exhibited a high affinity for BPA. Compared with other methods of detecting BPA[25, 26, 41], the prepared probe had great advantages, such as higher sensitivity, lower detection limit, and could be used to detect BPA in real samples.

The possible mechanism of fluorescence quenching

It was well known that fluorescence quenching included two quenching modes namely, dynamic and static quenching[48,49]. The fluorescence intensity of Fe_3O_4@SiO_2@QDs@MIPs NPs was decreased with the addition of the BPA (Fig. 3a), hence it could be deduced that fluorescence quenching should be static quenching[50,51]. The absorption and the emission spectrum of Fe_3O_4@SiO_2@QDs@MIPs NPs, Fe_3O_4@SiO_2@QDs@MIPs NPs with BPA are shown in Fig. 3b. The UV absorption band of Fe_3O_4@SiO_2@QDs@MIPs NPs in presence of BPA is close to the bandgap (curve 2), and has no spectral overlap with the emission spectrum of Fe_3O_4@SiO_2@QDs@MIPs NPs (curve 3). So the

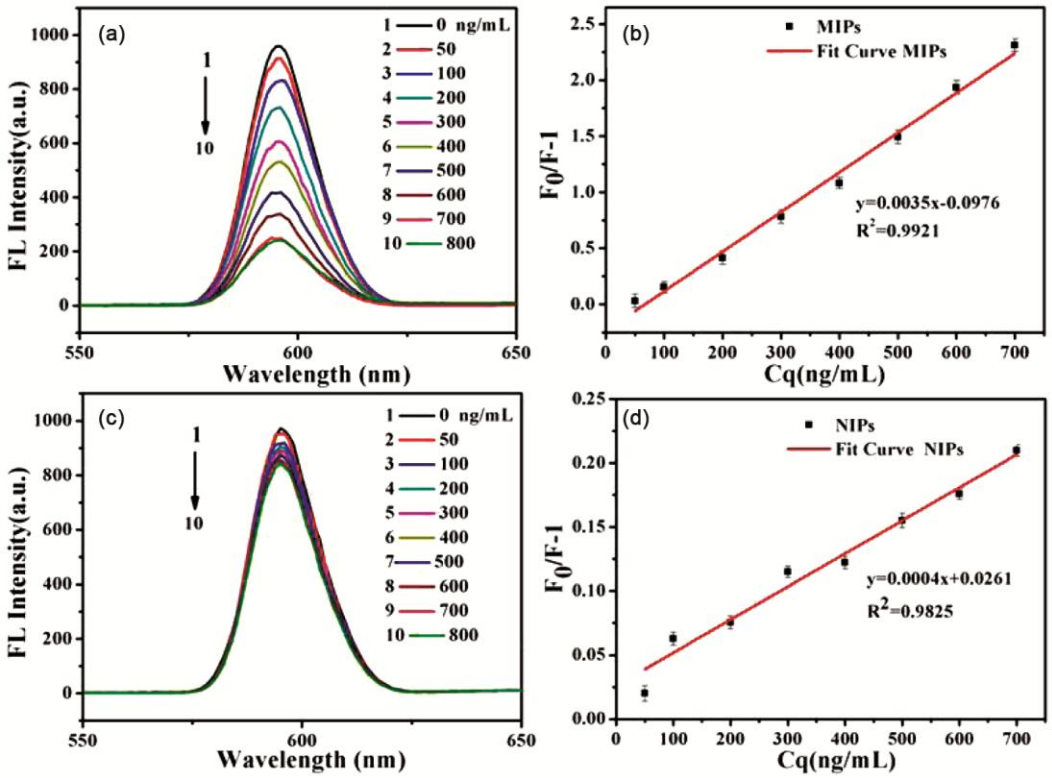

Fig. 2 — Fluorescence spectra of (a) Fe_3O_4@SiO_2@QDs@MIPs NPs and (c) Fe_3O_4@SiO_2@QDs@NIPs NPs versus concentration of BPA; Linear relationship between (b) Fe_3O_4@SiO_2@QDs@MIPs NPs and (d) Fe_3O_4@SiO_2@QDs@NIPs NPs versus concentration of BPA.

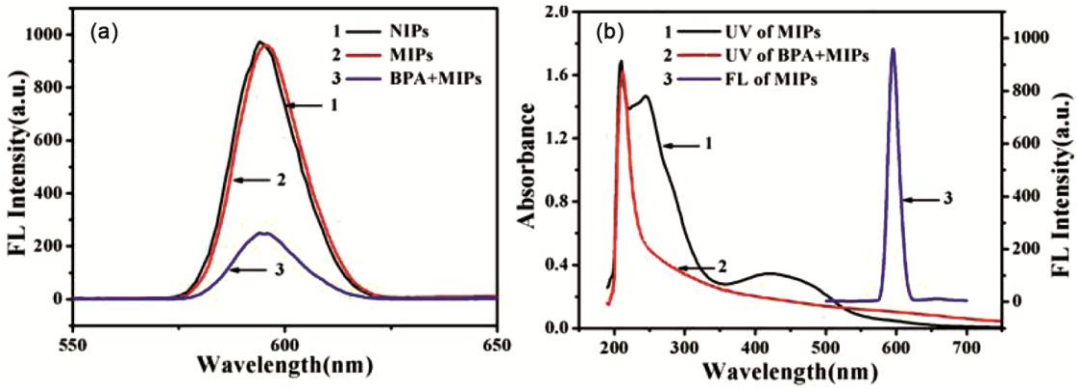

Fig. 3 — (a) The fluorescence spectra of Fe_3O_4@SiO_2@QDs@NIPs NPs (1), Fe_3O_4@SiO_2@QDs@MIPs NPs (2) and Fe_3O_4@SiO_2@QDs@MIPs NPs + BPA (3); (b) The UV spectra of Fe_3O_4@SiO_2@QDs@MIPs NPs (1), Fe_3O_4@SiO_2@QDs@MIPs NPs + BPA (2) and the fluorescence spectrum of Fe_3O_4@SiO_2@QDs@MIPs NPs (3).

energy transfer mechanism did not apply for this case. It was reported that a strong charge-transfer interaction could occur between the electron-deficient amino group and electron-rich aromatic ring (conjugating OH)[52,53]. The electron transfer would result in the formation of a complex between BPA and the amino group of Fe_3O_4@SiO_2@QDs@MIPs NPs on the surface of the QDs, then the photo-induced energy of QDs would be transferred to the complex resulting in fluorescence quenching of QDs.

An obvious difference was observed for the fluorescence spectra of the Fe_3O_4@SiO_2@QDs@MIPs NPs and Fe_3O_4@SiO_2@QDs@MIPs NPs rebinding BPA (Fig. 3a). The fluorescent intensity of Fe_3O_4@SiO_2@QDs@MIPs NPs in presence of BPA (curve 3) was weak which may be attributed to the electron transfer between Mn:ZnS QDs and BPA, the

Table 1 — Result for the detection of BPA in human urine

Sample	Spiked (ng/mL)	Found (ng/mL)	Recovery (%)	RSD (%) (n = 6)
Urine	100	99.94	99.94	2.19
	300	300.32	100.10	1.56
	500	500.91	100.18	2.11
	600	600.89	100.15	1.45

phenomenon were similar to that previously reported[51,54]. But the fluorescent intensity was restored after removing of BPA (curve 2) and was close to that of Fe_3O_4@SiO_2@QDs@NIPs NPs (curve 1), which also demonstrated that the template molecule was removed completely.

Analytical application

The practical feasibility of the prepared probe was applied to detect BPA in human urine. The concentrations of BPA in urine can reflect the human endocrine function in the body, and accurate determination of the content of BPA in urine is very important and useful. The results are shown in Table 1 and recoveries of the spiked samples showed that the method had good repetition, high accuracy and was simple and rapid. The average recovery was in the range of 99.94-100.18%, and the relative standard deviation was less than 2.19%, which indicates the proposed probe is very useful.

Conclusions

A fluorescence probe based on a hybrid Fe_3O_4@SiO_2@QDs@MIPs NPs was prepared successfully, and applied to detect the content of BPA in human urine sample. The silica structure and suitable shape of the material could reduce the mass transfer resistance and improved the sensitivity of fluorescence probe. The selective recognition to BPA was improved by the molecular imprinting technique. The method also had some advantages including low cost, simple preparation, good stability, and less time-consuming. The possible mechanism of fluorescence quenching was also studied. Fe_3O_4@SiO_2@QDs@MIPs NPs could rebinding selectively with the target molecule BPA, the transfer of electrons from electron-rich aromatic ring (conjugating OH) to electron-deficient amino group would result in the formation of a complex between BPA and the amino group of Fe_3O_4@SiO_2@QDs@MIPs NPs, then the photo-induced energy of QDs would be transferred to the complex which led to the fluorescence quenching of the Mn:ZnS QDs.

Supplementary Data

Supplementary data associated with this article are available in the electronic form at http://www.niscair.res.in/jinfo/ijca/IJCA_56A (07) 887-894_SupplData.pdf.

Acknowledgment

This work is supported by the National Natural Science Foundation of China (Nos. 20965007).

References

1 VomSaal F S & Hughes C, *Environ Health Perspect*, 11 (2005) 926.
2 Rosu D, Mustata F, Tudorachi N, Musteata V E, Rosua L & Varganicia C D, *RSC Adv*, 5 (2015) 45679.
3 Singh N, Reza K K, Ali M A, Agrawal V V & Biradar A M, *Biosens Bioelectron*, 68 (2015) 633.
4 Chung E, Jeon J, Yu J, Lee C & Choo J, *Biosens Bioelectron*, 64 (2015) 560.
5 Wang X, Lu X B, Wu L D & Chen J P, *Biosens Bioelectron*, 65 (2015) 295.
6 Pan D, Gu Y, Lan H, Sun Y & Gao H, *Anal Chim Acta*, 853 (2015) 297.
7 Soto A M, Sonnenschein C, *Nat Rev Endocrinol*, 6 (2010) 363.
8 Wu L, Deng D, Jin J, Lu X & Chen J, *Biosens Bioelectron*, 35 (2012) 193.
9 Watabe Y, Kondo T, Imai H, Morita M, Tanaka N & Hosoya K, *Anal Chem*, 76 (2004) 105.
10 Gallart-Ayala H, Moyano E & Galceran M T, *Mass Spectrom Rev*, 29 (2010) 776.
11 Gallart-Ayala H, Moyano E & Galceran M T, *Anal Chim Acta*, 683 (2011) 227.
12 Gatidou G, Thomaidis N S, Stasinakis A S & Lekkas T D, *J Chromatogr A*, 1138 (2007) 32.
13 Ouchi K, Watanabe S, *J Chromatogr B*, 780 (2002) 365.
14 Wen Y, Zhou B S, Xu Y, Jin S W & Feng Y Q, *J Chromatogr A*, 1133 (2006) 21.
15 Cirillo T, Latini G, Castaldi M A, Dipaola L, Fasano E, Esposito F, Scognamiglio G, Francesco F D & Cobellis L, *J Agric Food Chem*, 63 (2015) 3303.
16 Rezaee M, Yamini Y, Shariati S, Esrafili A & Shamsipur M, *J Chromatogr A*, 1216 (2009) 1511.
17 Rahman M M, Marwani H M, Asiri A M & Danish E Y, *Sens Bio-Sens Res*, 4 (2015) 70.
18 Wang F, Yang J & Wu K, *Anal Chim Acta*, 638 (2009) 23.
19 Yin H S, Zhou Y L & Ai S Y, *J Electroanal Chem*, 626 (2009) 80.
20 H. Yin, L. Cui, S. Ai, H. Fan & L. Zhu, *Electrochim Acta*, 55 (2010) 603.
21 Zhao J, Ma Y, Hou X, Li L, Zheng P & Li C, *J Solid State Electrochem*, 19 (2015) 15.
22 Ma M, Tu X, Zhan G, Li C & Zhang S, *Microchim Acta*, 181 (2014) 565.
23 Xu X, Zheng Q, Bai G, Song L, Yao Y, Cao X, Liu S & Yao C, *Electrochim Acta*, 242 (2017) 56.
24 Feng Y, Ning B, Su P, Wang H, Wang C, Chen F & Gao Z, *Talanta*, 80 (2009) 803.

25 Messaoud N B, Ghica M E, Dridi C, Ali M B & Christopher M A Brett, *Talanta*, 184 (2018) 388.
26 Li Y, Xu J Y, Wang L K, Huang Y J, Guo J J, Cao X Y, Shen F, Luo Y L & Sun C Y, *Sens Actuators B*, 222 (2016) 815.
27 Liu L, Fu H Y, Chen F, Ni C, Wang J X, Yin Q B, Mu Q L, Yang T M & She Y B, *Anal Chim Acta*, 963 (2017) 119.
28 Lv X X, Li Z Z, Niu C G, Ruan M, Huang D W & Zeng G M, *Water Sci Technol*, 66 (2012) 1361.
29 Li J H, Zhang Z, Xu S F, Chen L X, Zhou N, Xiong H & Peng H L, *J Mater Chem*, 21 (2011) 19267.
30 Chen L X, S.F. Xu, J.H. Li, *Chem Soc Rev*, 40 (2011) 2922.
31 Suriyanarayanan S, Cywinski P J, Moro A J, Mohr G J & Kutner W, *Top Curr Chem*, 325 (2012) 165.
32 Fuchs Y, Soppera O & Haupt K, *Anal Chim Acta*, 717 (2012) 7.
33 Alexander C, Andersson H S, Andersson L I, Ansell R J, Kirsch N & Nicholls I A, *J Mater Res*, 19 (2006) 106.
34 Yang Y Q, He X W, Wang Y Z, Li W Y & Zhang Y, *Biosen. Bioelectron*, 54 (2014) 266.
35 Tan L, Huang C, Peng R F, Tang Y W & Li W, *Biosens Bioelectron*, 61 (2014) 506.
36 Liu H L, Fang G Z & Wang S, *Biosens Bioelectron*, 55 (2014) 127.
37 Zhang L, Chen L, *ACS Appl Mater Interfaces*, 8 (2016) 16248.
38 Aliofkhazraei M, Ali N, *Mater Process*, 3 (2014) 245.
39 Zhou Y, Qu Z B, Zeng Y B, Zhou T S & Shi G Y, 52 (2014) 317.
40 Haun J B, Yoon T J, Lee H & Weisssleder R, *Nanomed Nanobiotechnol*, 2 (2010) 291.
41 Li M K, Hu L Y, Niu C G, Huang D W & Zeng G M, *Sens Actuators B*, 266 (2018) 805.
42 Hassan A H A, Moura S L, Ali F H M, Moselhy W A, Sotomayor M P T & Pividori M I, *Biosens Bioelectron*, 118 (2018) 181.
43 Zhao Y Y, Ma Y X, Li H & Wang L Y, *Anal Chem*, 84 (2012) 386.
44 Wang Z H, Zhang Y F, Zhang B & Lu X Q, *Talanta*, 190 (2018) 1.
45 Wang B, Hai J & Liu Z, *Angew Chem Int Ed*, 49 (2010) 4576.
46 Chen L Y, Chen C L, Li R N, Li Y & Liu S Q, *Chem Commun*, 19 (2009) 2670.
47 Lin Z, Xia Z W, Zheng J N, Zheng D, Zhang L, Yang H H & Chen G N, *J Mater Chem*, 22 (2012) 17914.
48 Kamat B P & Seetharamappa J, *J Chem Sci*, 117 (2005) 649.
49 Cheng P P H, Silvester D, Wang G L, Kalyuzhny G, Douglas A & Murray R W, *J Phys Chem B*, 110 (2006) 4637.
50 Chen Y F, Rosenzweig Z, *Anal Chem*, 74 (2002) 5132.
51 Wang H F, He Y, Ji T R & Yan X P, *Anal Chem*, 81 (2009) 1615.
52 Gunnlaugsson T, Kruger P E, Lee T C, Parkesh R, Pfeffer F M & Hussey G M, *Tetrahedron Lett*, 44 (2003) 6575.
53 Colpa J P, MacLean C & Mackor E L, *Tetrahedron*, 19 (1963) 65.
54 Tu R Y, Liu B H, Wang Z Y, Gao D M, Wang F, Fang Q L & Zhang Z P, *Anal Chem*, 80 (2008) 3458.